

AD-A065 006

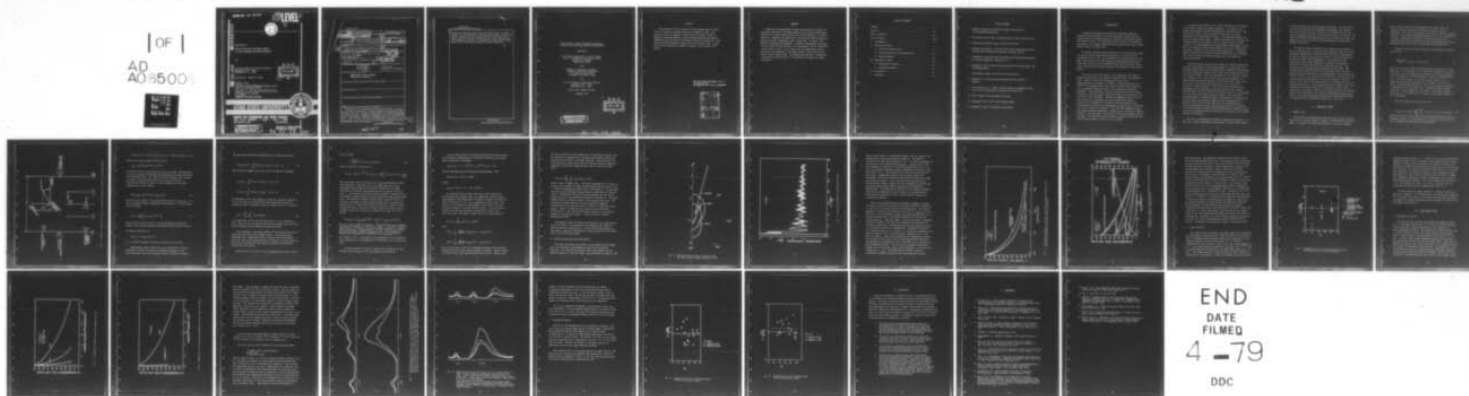
UTAH STATE UNIV LOGAN CENTER FOR ATMOSPHERIC AND SPA--ETC F/G 17/4
STUDY OF RADIATIVE SCATTERING CONCEPT OF PLUME INFRARED RADIATI--ETC(U)
DEC 78 R D HARRIS, K O'DELL, G G PIPPIN F49620-77-C-0121

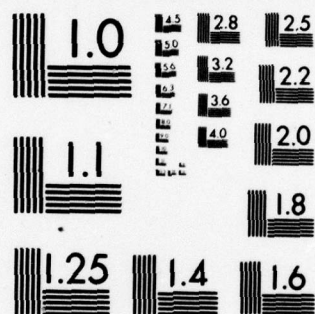
UNCLASSIFIED

AFOSR-TR-79-0039

NL

1 OF 1
AD
A065006





MICROCOPY RESOLUTION TEST CHART
NATIONAL BUREAU OF STANDARDS-1963-A

AFOSR-TR- 79-0039

(13) LEVEL II

ADA065006

DDC FILE COPY



Final Report:

STUDY OF RADIATIVE SCATTERING CONCEPT
OF PLUME INFRARED RADIATION OBSCURATION

for

Air Force Office of Scientific Research
Bolling Air Force Base
Washington D.C., 20332

Contract No. F49620-77-C-0121

December, 1978

AIR FORCE OFFICE OF SCIENTIFIC RESEARCH (AFSC)
NOTICE OF TRANSMITTAL TO DDC
This technical report has been reviewed and is
approved for public release IAW AFR 190-12 (7b).
Distribution is unlimited.

A. D. BLOSE
Technical Information Officer

DDC
RECEIVED
FEB 28 1979
B

UTAH STATE UNIVERSITY



CENTER FOR ATMOSPHERIC AND SPACE SCIENCES
UTAH STATE UNIVERSITY • LOGAN • UTAH • 84322
(801) 752-4100, EXT. 7878
TELEX 9109715876

DISTRIBUTION STATEMENT A
Approved for public release
Distribution Unlimited

Approved for public release
distribution unlimited.

79 02 16 090

UNCLASSIFIED

SECURITY CLASSIFICATION OF THIS PAGE (When Data Entered)

1. REPORT DOCUMENTATION PAGE		READ INSTRUCTIONS BEFORE COMPLETING FORM	
18	2. REPORT NUMBER AFOSR-TR-79-0039	3. GOVT ACCESSION NO.	4. RECIPIENT'S CATALOG NUMBER
5. TITLE (and Subtitle) Study of Radiative Scattering Concept of Plume Infrared Radiation Obscuration.		6. AUTHOR(s) R.D./Harris, Keith/O'Dell, G.G./Pippin, Stephen J./Young, L.R./Martin	
7. PERFORMING ORGANIZATION NAME AND ADDRESS Center for Atmospheric and Space Sciences, Utah State University, Logan, Utah 84322		8. CONTRACT OR GRANT NUMBER(s) F49620-77-C-0121	
9. CONTROLLING OFFICE NAME AND ADDRESS Air Force Office of Scientific Research Bldg. 410 NP Bolling AFB, Washington, D.C. 20332		10. PROGRAM ELEMENT, PROJECT, TASK AREA & WORK UNIT NUMBERS 61102F 2301 A5	
11. MONITORING AGENCY NAME AND ADDRESS (if different from 9)		12. REPORT DATE December 1978	
13. SECURITY CLASS (of this report) Unclassified		14. DECLASSIFICATION DOWNGRADING SCHEDULE	
15. DISTRIBUTION STATEMENT (of this Report) Approved for public release; distribution unlimited.			
16. DISTRIBUTION STATEMENT (of the abstract entered in Block 20, if different from Report)			
17. SUPPLEMENTARY NOTES			
18. KEY WORDS (Continue on reverse side if necessary and identify by block number)			
19. ABSTRACT (Continue on reverse side if necessary and identify by block number) Theoretical and experimental studies were performed to measure the synergistic absorption of hot-gas radiation by an aerosol/absorbing gas mixture and to verify quantitatively the infrared absorption of carbon particles. Computer calculations for a pure scatterer/N ₂ O absorbing gas mixture revealed a synergistic effect of only 10%. In carbon - N ₂ O mixtures, synergism was negligible. Attenuation meas-			

DD FORM 1 JAN 73 1473 EDITION OF 1 NOV 65 IS OBSOLETE

UNCLASSIFIED

SECURITY CLASSIFICATION OF THIS PAGE (When Data Entered)

411 067

LB

→ next page

UNCLASSIFIED

SECURITY CLASSIFICATION OF THIS PAGE(When Data Entered)

Measurements were made for pure carbon and TiO_2 aerosols, pure N_2O samples, and the combination of each aerosol in N_2O . In all cases, the net transmittance of the gas/aerosol was described by the simple product of the N_2O alone and aerosol alone transmittances. No synergism were detected. Transmission calculations for carbon show it a very effective candidate for plume obscuration.

UNCLASSIFIED

SECURITY CLASSIFICATION OF THIS PAGE(When Data Entered)

**Final Report: Study of Radiative Scattering
Concept of Plume Infrared Radiation Obscuration**

Prepared by

**R.D. Harris, Keith O'Dell, and G.G. Pippin
Center for Atmospheric and Space Sciences
Utah State University
Logan, Utah 84322**

and

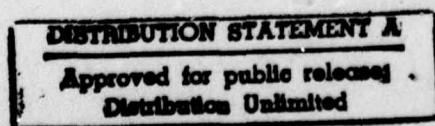
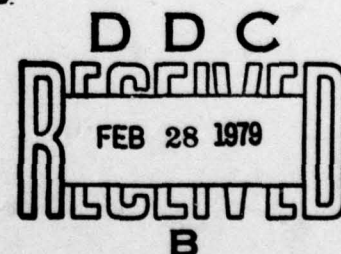
**Stephen J. Young and L.R. Martin
Chemistry and Physics Laboratory
The Aerospace Corporation
El Segundo, California 90245**

for

**Air Force Office of Scientific Research
Bolling Air Force Base
Washington D.C., 20332**

Contract No. F49620-77-C-0121

December 1978



Foreward

This document is a final report of work performed under Air Force Office of Scientific Research Contract No. F49620-77-C-0121. The contract was let in response to the unsolicited proposal "Study of Radiative Scattering Concept of Plume Infrared Radiation Obscuration" submitted to the Air Force by Utah State University in March 1977. The work was performed between 1 August 1977 and 30 October 1978. A three month no-cost extension enlarged the original 1 year contract to 15 months.

RE: Classified references, distribution unlimited-
No change per Ms. Biese, AFOSR/XOPD

ACCESSION for		
NTIS	White Section	<input checked="checked" type="checkbox"/>
DDC	Buff Section	<input type="checkbox"/>
UNANNOUNCED		<input type="checkbox"/>
JUSTIFICATION		
BY		
DISTRIBUTION/AVAILABILITY CODES		
Dist.	AVAIL. and/or	SPECIAL
A		

ABSTRACT

Theoretical and experimental studies were performed to measure the synergistic absorption of hot-gas radiation by an aerosol/absorbing gas mixture and to verify quantitatively the infrared absorption of carbon particles. Computer calculations for a pure scatterer/ N_2O absorbing gas mixture revealed a synergistic effect of only 10%. In carbon - N_2O mixtures, synergism was negligible. Attenuation measurements were made for pure carbon and TiO_2 aerosols, pure N_2O samples, and the combination of each aerosol in N_2O . In all cases, the net transmittance of the gas/aerosol was described by the simple product of the N_2O alone and aerosol alone transmittances. No synergism was detected. Transmission calculations for carbon show it a very effective candidate for plume obscuration.

TABLE OF CONTENTS

Forward	<i>i</i>
Abstract	<i>ii</i>
Table of Contents	<i>iii</i>
List of Figures	<i>iiii</i>
I. Introduction	1
II. Theoretical Effort	3
A. Scattering Computer Code	3
B. Scattering Particles and Absorbing Gas	10
C. Carbon Absorption	16
III. Experimental Effort	18
A. Experimental Procedure	18
B. Experimental Results	24
IV. Conclusions	27
V. References	28

LIST OF FIGURES

1. Schematic diagram for radiation transport calculation in scattering/absorbing medium.
2. Mie phase function versus scattering angle for three particle sizes.
3. Scattering coefficient (Q_{sct}) versus particle size.
4. Transmission through a 1 km thick slab of pure scattering particles for both uni-directional and isotropic radiation sources.
5. Transmission values for pure scattering and/or N_2O absorbing mediums to evaluate synergistic effects at $x = .1$.
6. Synergistic ratio for pure scattering particles and N_2O mixture, and carbon- N_2O mixture.
7. Transmission through 1 km slab of carbon particles.
8. Comparison of carbon and N_2O transmissions versus weight of absorber.
9. Flame spectrum, $4.1 - 4.8\mu\text{m}$, as seen through CO_2 atmospheric path and 20 torr of N_2O /carbon or N_2 /carbon scattering cell.
10. Same as Figure 9 but with 600 torr of N_2O .
11. Synergistic ratio for 0.3 micron carbon sample.
12. Synergistic ratio for $2\mu\text{m}$ micron TiO_2 sample.

I. INTRODUCTION

A combined experimental and theoretical (modeling) program to determine the effectiveness of aerosol scattering to reduce infrared radiation from jet engine exhausts was carried out under AFOSR contract No. F49620-77-C-0121. The experimental work was done at the Aerospace Corporation in El Segundo, California and the theoretical effort at Utah State University in Logan, Utah.

The primary infrared emission features of jet engine exhaust plumes are the CO_2 and H_2O vibration/rotation bands at $2.7\mu\text{m}$ and the CO_2 fundamental band at $4.3\mu\text{m}$. The intensities of these emissions are very high, particularly for aircraft operating in the augmented-power mode where they may be an order of magnitude higher than at military power levels, and provide the primary signal for the guidance of heat seeking missiles.

The natural CO_2 and H_2O content of the atmosphere can provide a significant reduction in the emission intensities over long atmospheric paths. However, because the emission bands arise from a high-temperature environment ($T \approx 900^\circ\text{K}$ for military power and up to 2100°K in the augmented power mode) they are substantially wider than the corresponding absorption bands of the relatively cool ambient atmosphere. This widening is caused by the population of both higher vibrational levels and higher rotational levels of the molecules in the plume than in the atmosphere. Whereas the atmospheric CO_2 and H_2O are very effective at attenuating the plume emission band centers, essentially no attenuation is provided in the band wings and this "wing-leakage" radiation can be propagated over many miles of atmosphere with little reduction in intensity. Over very long atmospheric paths, the radiated spectrum approaches a limiting form of very sharp intensity "spikes" at the band edges, particularly on the short-wavelength side of the bands. The principle spectral regions of concern are thus the red- and blue-spike regions of the 2.7 and $4.3\mu\text{m}$ bands.

A previous study [Harris et al., 1975] considered the obscuration of this spike radiation by gaseous absorption. In concept, a cool gaseous shroud would be formed aerodynamically around the plume. The shroud would contain a gas or mixture of gases that had strong absorption in the spike spectral regions. An experimental search was made for suitable shroud gases. Several candidates were found which had reasonable obscuration potential for one or more of the four spike features. The prime examples were H_2O and methyl isothiocyanate for the N_2O $4.6\mu m$ CO_2 band wing and N_2O and formic acid for the $2.9\mu m$ H_2O/CO_2 band wing. Estimates of the amount of these materials (hundreds of pounds) that would be required to provide a 90% reduction of intensity for a period of about 10 seconds indicated that the concept was marginally feasible.

Infrared radiation reduction was reported for aircraft plumes when an aerosol suspension of particles was formed as a shroud around the aircraft exhaust plume or in the plume itself. Obscuration was reported for carbon suspensions [Varney, 1972; Blozy, 1974; Birstein, 1976], oil mist shrouds [Varney, 1972], and purportedly for jet fuel mists [Varney, 1972; Caldwell, 1975]. The fact that these techniques employed an aerosol suspension of particulates or liquid drops would suggest that the effects of radiation scattering play a role in the overall obscuration effects observed. It should be clearly stated, however, that pure scattering phenomena could not account for an intensity reduction when the field of view of the observing sensor is large enough to include the entire plume and aerosol shroud. For a cylindrical shrouding geometry in which the plume is surrounded on all sides by the aerosol shroud, the extinction effects of side and backscatter by a particular small volume of the shroud must be cancelled when the scattering contribution of all such scattering volumes is considered. (A small percentage of radiation could conceivably be "funnelled" to the rear of the cylindrical shroud if this end is not filled in by turbulent closing of the shroud.)

The only real mechanism for radiation reduction is absorption. In the case of carbon suspensions, the absorption is evident since carbon

is black throughout the infrared region of interest. For the oil mist and fuel mist techniques, the suppression mechanism is not entirely clear since neither jet fuel (kerosene) nor presumably the oils used provide significant absorption in the infrared regions of interest. The suspected mechanism for these suppressants is that they do provide some absorption and that the effects of scattering tend to enhance this absorptive potential.

The specific question addressed in the present work is whether or not the superposition of a gas and aerosol suspension might result in a synergistic enhancement of absorption such that the net transmittance through the mixture is less than the product of the transmittances of the gas and aerosol taken independently. Both theoretical and experimental efforts were undertaken to evaluate any synergistic absorptions that might be produced by scattering particles. Two particle types were considered; titanium dioxide and carbon. The transparency of titanium dioxide in the infrared allows a study of purely scattering interactions in an absorbing gas. N_2O was chosen for this gas because of its relatively good absorption in both the 2.9 and 4.6 μm regions and because of its ease of handling. The other particle type, carbon, was chosen because of its absorptive as well as scattering properties. A brief description of the computer code used to theoretically calculate scattering is followed by results aimed at evaluating the synergistic effects of scattering particles and absorbing gases, and calculations of the radiation transmission through carbon. Results of radiation measurements through scattering/absorbing mediums are presented next followed by the conclusions of this work.

II. THEORETICAL EFFORT

A. Computer Code

The theoretical work performed under this contract dealt with the calculation of infrared radiation through a scattering and/or absorbing medium. A computer code based on the Braslau - Dave solar radiation

model [Braslau and Dave, 1973] and modified by Luther [1974] was obtained from the University of California, Lawrence Livermore Laboratory. This code was developed to calculate the vertical radiation transport in the scattering/absorbing portion of the lower atmosphere of the earth. Modifications were made at Utah State University to calculate the infrared transmission through a one-dimensional horizontal homogeneous path filled with scattering and absorbing particles.

The basic radiative transfer equation for monochromatic radiation has the form

$$\frac{dI(\tau; \mu, \phi)}{d\tau} = I(\tau; \mu, \phi) - w(\tau)J(\tau; \mu, \phi) \quad (1)$$

where $I(\tau; \mu, \phi)$ is the intensity of the radiation at position τ in the direction $\mu = \cos \theta$, ϕ where θ is the angle with respect to the normal to the slab and ϕ is the azimuth angle referred to an arbitrary meridian plane (see Figure 1). Forward (backward) direction is represented by $+\mu$ ($-\mu$). The optical depth τ is the sum of optical depths due to absorption and scattering processes and is defined to be 0 at the source, increasing into the medium. Values for the scattering depth can be computed by Mie theory [Dave, 1974]. Absorption optical depths depend upon the gas absorption cross section. The albedo of single scattering $w(\tau)$ is defined as $w(\tau) = \Delta\tau^s / \Delta\tau$ the fractional change in τ due to scattering.

The source function $J(\tau; \mu, \phi)$ is given by

$$J(\tau; \mu, \phi) = B(\tau, \mu, \phi) + \frac{1}{4\pi} \int_{-1}^{+1} \int_0^{2\pi} P(\tau; \mu, \phi; \mu', \phi') I(\tau, \mu', \phi') d\mu' d\phi' \quad (2)$$

where $P(\tau; \mu, \phi; \mu', \phi')$ is the phase function which describes the amount of radiation scattered into the direction (μ, ϕ) from the direction (μ', ϕ') . For our purposes the phase function can be written

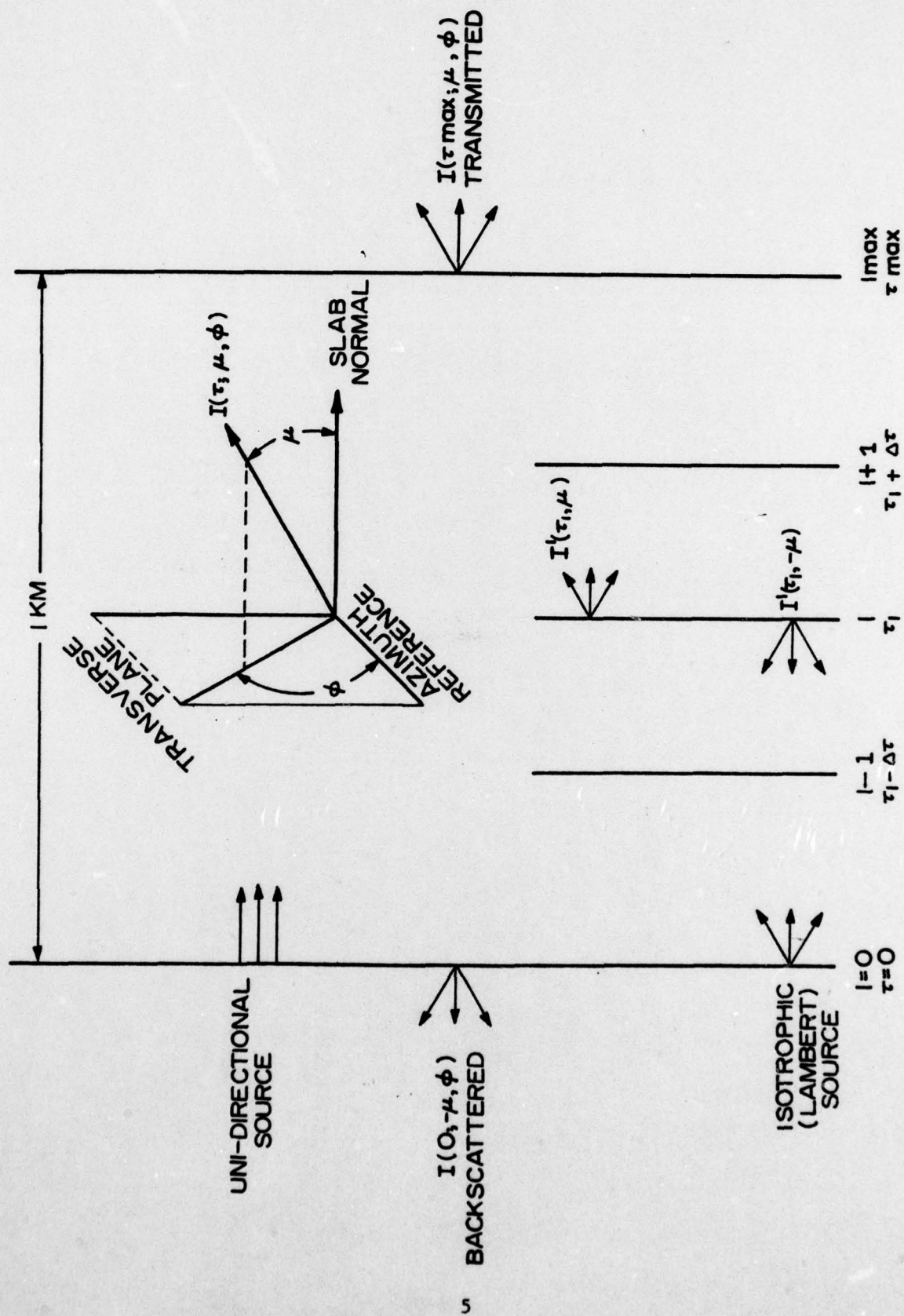


Fig. 1. Schematic diagram for radiation transport calculation in scattering/absorbing medium.

$$P(\tau; \mu, \phi; \mu', \phi') = T(\tau) M(\mu, \phi; \mu', \phi') + (1 - T(\tau)) R(\mu, \phi; \mu', \phi') \quad (3)$$

where the so called turbidity factor $T(\tau)$ is

$$T(\tau) = \Delta\tau^{(s,m)} / (\Delta\tau^{(s,m)} + \Delta\tau^{(s,r)})$$

the fraction of total scattering due to Mie scattering. The quantities M and R are the Mie and Rayleigh scattering phase functions respectively to be described later. The B function for our radiation model stands for either a unidirectional source or an isotropic radiator. A unidirectional source is similar to solar radiation in the earth's atmosphere and can be written

$$B(\tau; \mu_0, \phi_0) = \frac{1}{4} e^{-\tau/\mu_0} P(\tau; \mu, \phi; \mu', \phi') F \quad (4)$$

where πF is the incident flux (watts/cm²- μm) normal to (μ_0, ϕ_0) at $\tau = 0$. For an isotropic radiator (Lambertian illumination) at $\tau = 0$ the source function becomes

$$B(\tau; \mu) = \frac{1}{2} \int_0^1 P(\tau; \mu, \mu_1) e^{-\tau/\mu_1} d\mu_1 \quad (5)$$

These formulas are only strictly true for monochromatic radiation, however, with suitable averages a wavelength interval may be simulated.

The boundary conditions are

$$I(0; \mu, \phi) = I(\tau_{\max}; -\mu, \phi) = 0$$

i.e., no diffuse radiation incident at either end of the slab.

Chandrasekhar [1960] showed that if the phase function could be expressed in a Taylor-like-series of Legendre polynomials in the scattering angle, then by the addition theorem of spherical harmonics

the phase function could be represented in the Fourier series form

$$P(\tau; \mu, \phi; \mu', \phi') = \sum_{n=1}^N P^n(T; \mu, \mu') \cos(n-1) (\phi' - \phi) \quad (6)$$

This form for P suggests that I and J could be similarly expanded

$$I(\tau; \mu, \phi) = \sum_{n=1}^N I^n(\tau; \mu, \mu') \cos(n-1) (\phi' - \phi)$$

$$J(\tau; \mu, \phi) = \sum_{n=1}^N J^n(T; \mu, \mu') \cos(n-1) (\phi' - \phi) \quad (7)$$

The advantage of this type expansion is that the azimuthal integral in (2) can be carried out analytically with considerable reduction in computation time. Furthermore, since the forward flux at τ is given by

$$F_f(\tau) = \int_0^{2\pi} \int_0^{1*} I(\tau; \mu, \phi) \mu d\mu d\phi \quad (8)$$

if we substitute (7) into (8) all terms with $n > 1$ will integrate to zero. Thus, for flux calculations we need only consider one term in the Fourier expansion of the intensity and phase functions.

From a distance, a jet engine exhaust has characteristics of both a mono-directional source and a Lambert source. The exhaust gasses undoubtedly emit isotropically but at a distance only those photons which come from a small steradian will be detected. For this reason we have made calculations with both sources to bracket the conditions existing for real sources.

Substituting $\phi' = \phi_0$ into (7) for a monodirectional source, and (7)

into (1) gives

$$\mu \frac{dI^1(\tau, \mu)}{d\tau} = I^1(\tau, \mu) - w(\tau)J^1(\tau, \mu) \quad (9)$$

where J^1 from (2), (4) and (6) is

$$J^1(\tau, \mu) = 1/4 F e^{-\tau/\mu_0} P^1(\tau; \mu, \mu_0) + 1/2 \int_{-1}^1 P^1(\tau, \mu, \mu') I^1(\tau, \mu') d\mu' \quad (10)$$

Each term of (9) and (10) has a $\cos(n-1)(\phi_0 - \phi)$ multiplying it which can be neglected. The first term on the right hand side of (10) represents the contribution to the source function due to primary scattering of the direct unidirectional source by the unit volume at level τ . A successive scattering iteration procedure is used to solve the radiative transfer equation (9) using this first term as the initial value. The iteration procedure continues until values of $I^1(\tau, \mu)$ on successive iterations converge to some tolerance for all values of μ . Numerically (9) is solved by dividing the slab into a number of layers. Assuming the value of the source function within each layer to be the arithmetic mean of the values at the edges of the layer, (9) can be written

$$I^1(\tau_k; \pm\mu) = I^1(\tau_{k+1}; \pm\mu) e^{-\Delta\tau_k/\mu} - w(\tau_k) J^1(\tau_k; \pm\mu) [1 - e^{-\Delta\tau_k/\mu}]$$

where $k = l$ for $+\mu$ and $k = l-1$ for $-\mu$. $I^1(\tau_k; \mu)$ and $I^1(\tau_k; -\mu)$ represent the intensities emergent at the front of layer $l-1$ and back of layer l respectively. All values of $I^1(\tau_k; +\mu)$, forward direction, are computed before proceeding to computations of $I^1(\tau_k; -\mu)$. This means a forward pass from the source outward (increasing l) for $I^1(\tau, \mu)$ and then a backward pass (decreasing l) through the slab calculating $I^1(\tau; -\mu)$.

The integral of (10) is evaluated by the trapezoidal rule of integration using increments of μ corresponding to 2° increments in θ (91 values per layer).

A similar procedure is used to calculate the intensities for the isotropic source but with (5) as the primary source function.

For very small particles (Rayleigh scattering) the phase function can be found by substituting the relationship between the scattering angle and spherical coordinates

$$\cos \theta = \mu \mu' + (1 - \mu^2)^{1/2} (1 - \mu'^2)^{1/2} \cos (\phi' - \phi)$$

into the Rayleigh scattering expression [Chandrasekhar, 1960]

$$R(u, \phi; u', \phi') = 3/4(1 + \cos^2 \theta)$$

to give

$$R(\mu, \mu') = 3/8 (3 - \mu^2 - \mu'^2 + 3\mu^2 \mu'^2)$$

The phase function for large particles is more involved and requires much more computer time. Mie [1908] first solved for the electromagnetic field scattered by a dielectric sphere, of radius and index of refraction $m = n_1 - in_2$, irradiated by a plane wave. The details of this problem in electromagnetic field theory are nicely described in Chapter 13 of Born and Wolf [1970]. It is sufficient to say here that the wave intensity scattered into a cone of unit solid angle whose axis makes an angle θ with the incident beam as

$$I(x, m, \theta) = \frac{\lambda^2}{8\pi^2} (S_1^2(\theta) + S_2^2(\theta))$$

where

$$S_1(\theta) = \sum_{n=1}^{\infty} \frac{2n+1}{n(n+1)} [a_n \pi_n(\cos \theta) + b_n \tau_n(\cos \theta)]$$

$$S_2(\theta) = \sum_{n=1}^{\infty} \frac{2n+1}{n(n+1)} [b_n \pi_n(\cos \theta) + a_n \tau_n(\cos \theta)]$$

and $\pi_n(\cos \theta)$ and $\tau_n(\cos \theta)$ are expressed in terms of the first and second derivatives of the ordinary Legendre functions. Compare Chapter 9 of Van De Hulst [1957] and Chu and Churchill [1955]. Sekera [1952]

and Chu and Churchill [1955] showed that the scattering functions could be simplified by repeated use of recurrent relationships between the derivatives and products of Legendre functions. This would yield for these functions a series whose terms are ordinary Legendre polynomials weighted by coefficients depending upon m and $x = 2\pi a/\lambda$ only [Dave, 1970;

$$I(x, m, \theta) = \frac{\lambda^2}{4\pi^2} \sum_{k=1}^N L_k(x, m) P_{k-1}(\cos \theta)$$

Dave J.V. and J. Gazdag, 1970]. The series converges for all values of x and m , but the number of terms required depends upon the size of x and m . Generally speaking the larger x and m , the greater N . The Mie phase function is then calculated by generating the L_k for specific values of x and m . The legendre functions are then calculated for the desired values of μ and μ' and the series evaluated to find $M(\mu, \mu')$. The phase function $M(\mu, 1)$ is plotted in figure 2 for three particle sizes. mie scattering for small particles is seen to approach a Rayleigh distribution and for large particles is primarily a forward scattering process. Figure 3 illustrates the variation of the scattering coefficient (i.e. the ratio of total power scattered to the particle geometric cross section) versus x . Similar curves are found in Deirmendjian [1969].

The computer code will actually calculate L_k 's for a distribution of particle sizes. The coefficients are weighted by the number of particles having the given size x . For the calculations presented in this report, a gaussian distribution of sizes was used with the extreme radii $\pm 5\%$ of the center radius.

B. Scattering Particles and Absorbing Gas

The first task was the calculation of the radiation flux emerging from a one kilometer thick homogeneous slab of pure scattering particles. The "effective" thickness of the slab depended upon the particle content of a one cm^2 column. The transmission through the slab

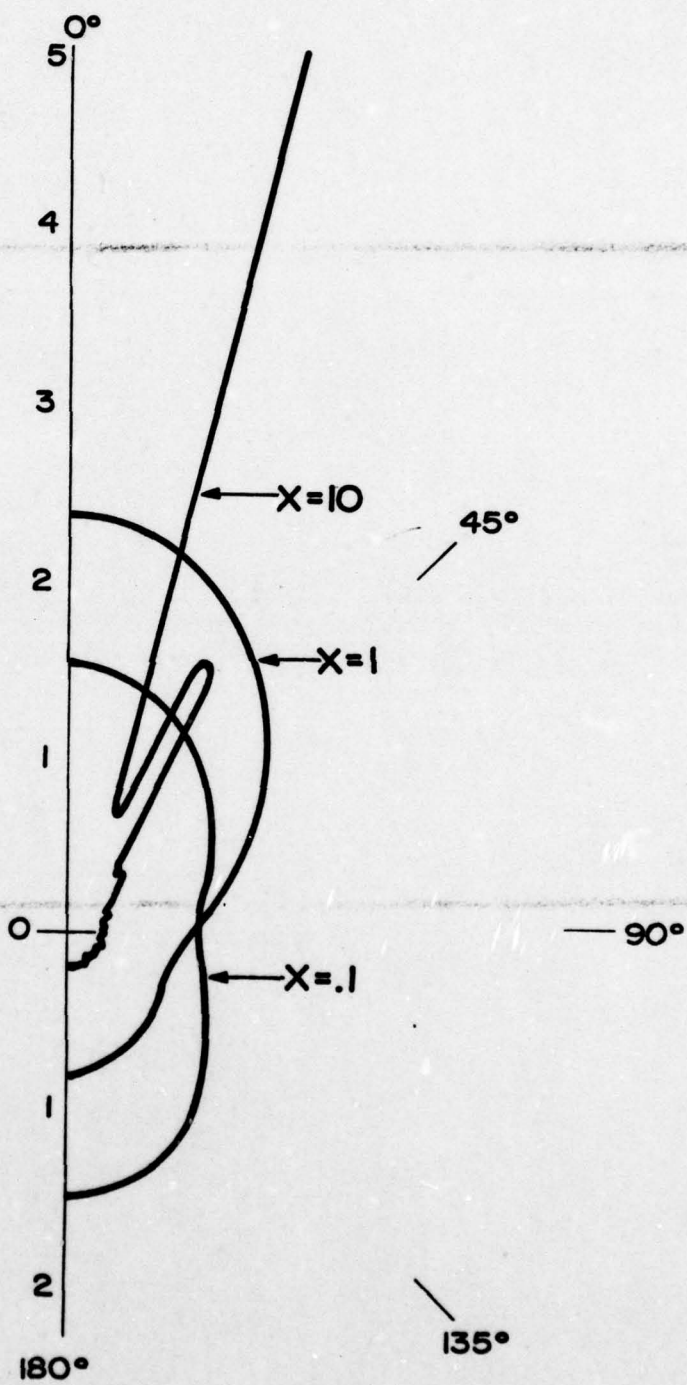


Fig. 2. Mie phase function versus scattering angle for three particle sizes, $X=2\pi r/\lambda=.1, 1, 10$.

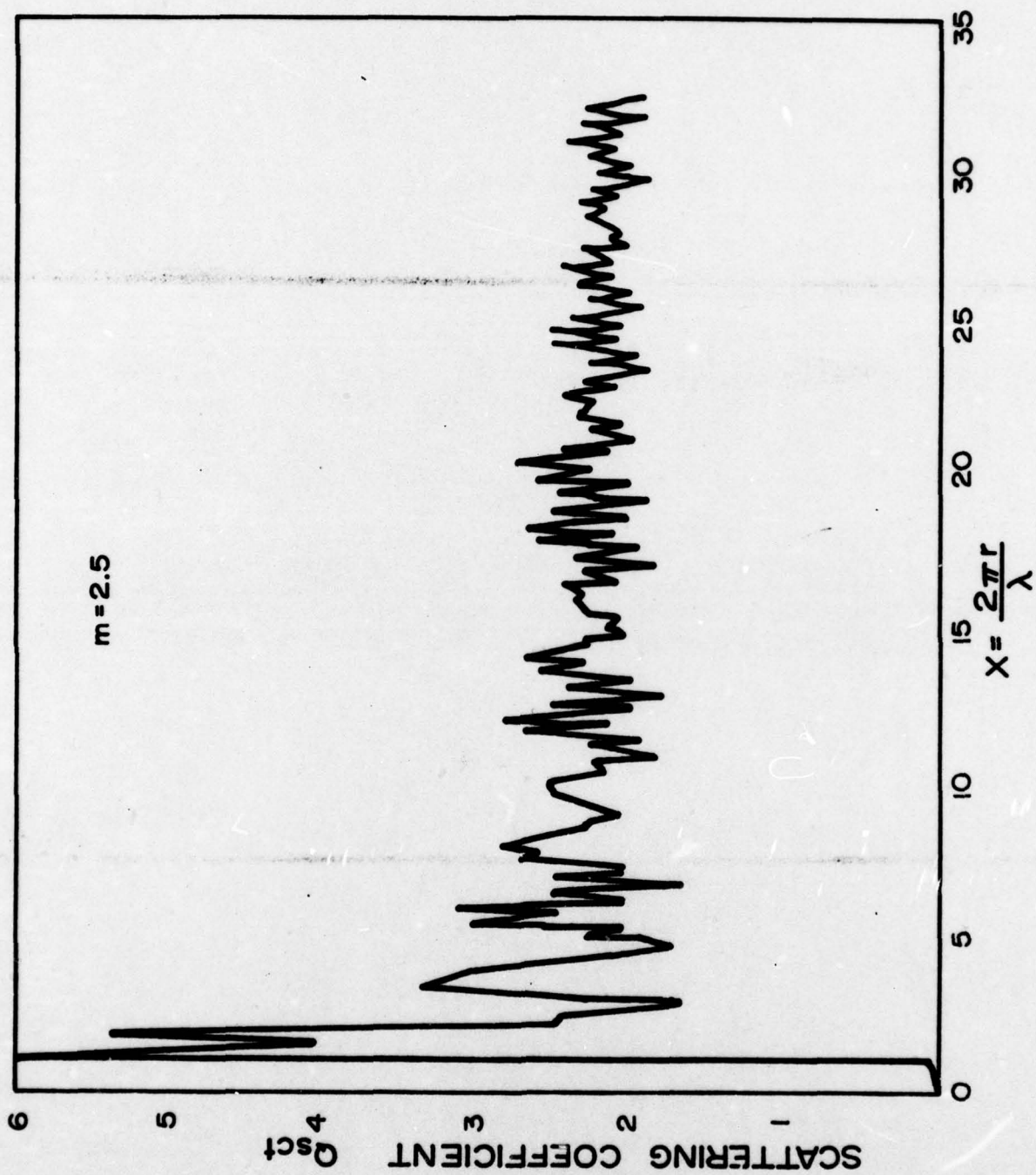


Fig. 3. Scattering coefficient versus particle size.

versus column content, or equivalently density, for the isotropic and mon-directional sources are plotted in Figure 4. The index of refraction for these calculations was $m = 2.7 + i0$, which corresponds to the real part of the carbon refractive index. Actually there is not much difference in the particle scattering effectiveness for $m > 2.5$, since the average scattering is almost independent of refractive index above about $m = 2.5$. The radiation flux at the source was equal for both cases. Transmission values for the isotropic source were consistently less than the monodirectional source because the average path length was greater. Since a purely scattering medium cannot destroy photons, Figure 4 implies that the transmission decreases with increasing optical depth because increasingly more radiation is backscattered. The backscattered radiation is the difference between 100% and the transmission, so that the sum of the transmitted and backscattered intensities is unity. This is just the statement of conservation of energy.

Based on these characteristics of radiation transport in a pure scatterer, our aim was to evaluate the possible synergistic absorption in a mixture of scattering particles and absorbing gas. The degree of synergism is defined as the amount that the ratio $R = \tau_{pg} / \tau_p \tau_g$ is less than unity. The transmission through scattering particles alone is τ_p , through absorbing gas τ_g , and through a mixture of scatterers and absorbing gas τ_{pg} . (The greek symbol τ has been used here to represent transmission whereas τ was used in the computer code description to represent optical depth.) Scattering particles were assumed to have $m = 2.7$ and N_2O was used for the absorbing gas. Transmission values for three particle sizes, $x = .1, 1$ and 10 . At $4.5\mu m$ this corresponded to a particle radius of $.72, 7.2$ and 72 microns. Results for $x = .1$ are shown in Figure 5. These curves illustrate the transmission through a one km thick slab for three values of scattering particle densities, corresponding to transmissions of 20, 50 and 80%, and as a function of N_2O absorbing gas density. The solid curves represent transmission through 1 km of scattering τ_p and 1 km of absorption τ_a , with the total transmission $\tau = \tau_p \tau_a$. The dashed curves in Figure 5 are the transmissions through a mixture of pure scattering particles and

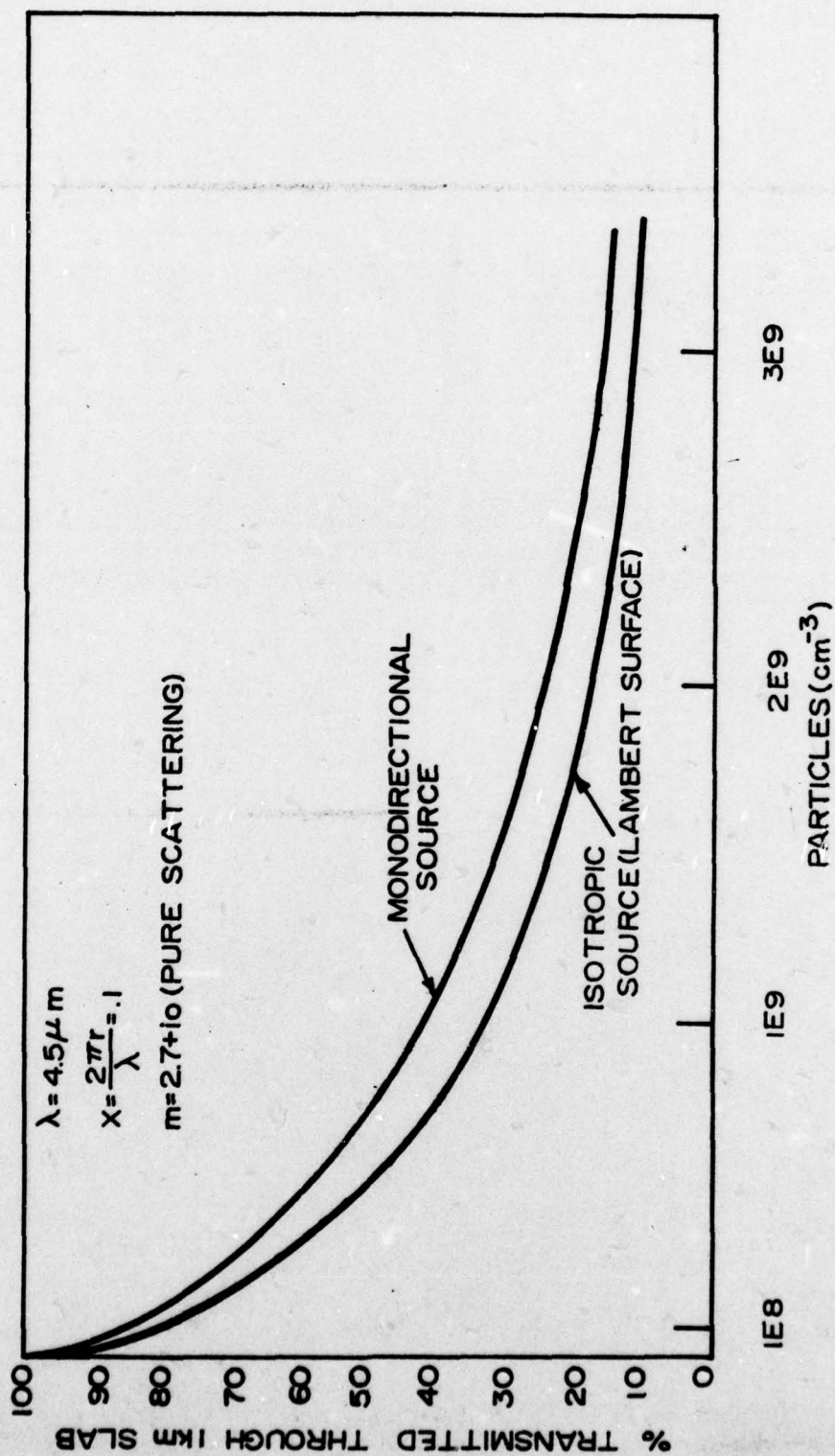


Fig. 4. Transmission through a 1 km thick slab of pure scattering particles for both uni-directional and isotropic radiation sources.

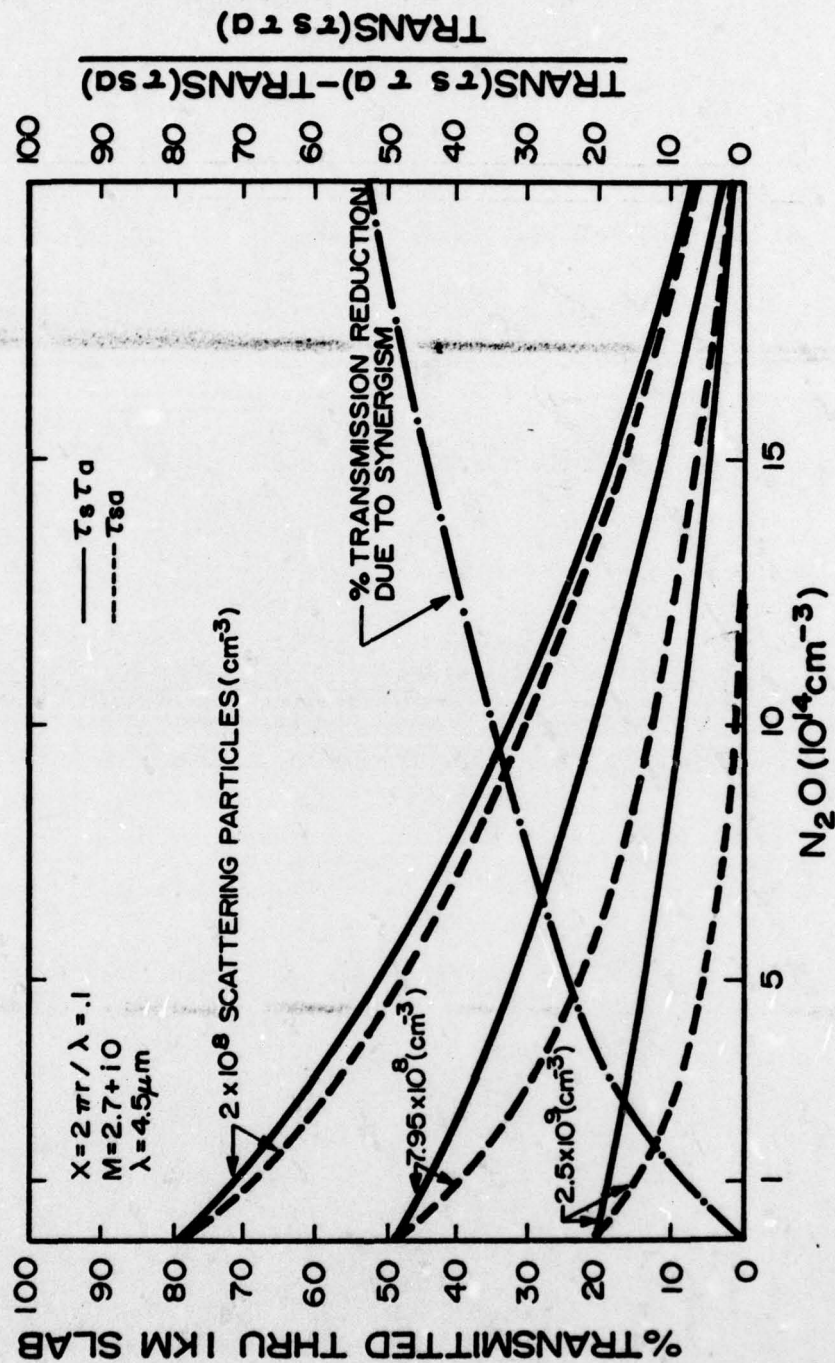


Fig. 5. Transmission values for pure scattering and/or N_2O absorbing mediums to evaluate synergistic effects at $x=.1$.

absorbing N_2O gas. The difference between these two sets of curves shows that some synergism does occur. On an absolute scale this effect is always less than 10%, which is not quite enough to be an attractive infrared obscuration technique. The dot dashed curve in Figure 5 and the synergism ratio R plotted in Figure 6 show that the percent reduction in transmission due to synergistic effects is greatest for small values of transmission (large absorption). However, these relative values are misleading. If we take a mixture of $7.95 \times 10^{18} \text{ cm}^{-3}$ scattering particles and $8 \times 10^{14} \text{ cm}^{-3}$ molecules of N_2O the curves show a transmission of 16% through a 1 km thick slab. For titanium dioxide scattering particles, this total number density would correspond to a total mass density of $5.06 \times 10^{-6} \text{ gm/cm}^3$, made up of $5 \times 10^{-6} \text{ gm/cm}^3$ for titanium dioxide and $6 \times 10^{-8} \text{ gm/cm}^3$ for N_2O . A density of 1.8×10^{15} molecules/ cm^3 of N_2O would also give a 16% transmission but would only weigh $1.3 \times 10^{-7} \text{ gm/cm}^3$. If kerosene had the same scattering properties it would only reduce the scattering particle weight by a factor of 4. We conclude from these calculations that pure spherical scattering particles added to an absorbing gas will decrease the infrared transmission through the gas, but unfortunately the effect is small and unless there is a very light weight scattering particle the combined weight of the scattering/absorbing mixture will exceed that of just an absorbing gas. Any hope to use this technique in plume IR obscuration will have to lie with scattering particles that absorb as well as scatter. We analyze one such particle, carbon, in the next section.

C. Carbon Absorption

The complex index of refraction for carbon leads to both absorption and scattering for carbon particles. Since the value of the refractive index is dependent upon the physical state of the carbon and also the wavelength [Whitson, 1975] we have used $m = 2.7 - i1$ which is representative of soot between 2.7 and 4.5 μm . For a size parameter of $x = .1$, the volume scattering coefficient is only $\beta_s = 2.5 \times 10^{-14}$ while the volume absorption coefficient is over 1000 times higher at $\beta_a = 1 \times 10^{-11}$. This simply means that carbon particles are more effective as absorbers than as scatterers. A series of computer runs were made with

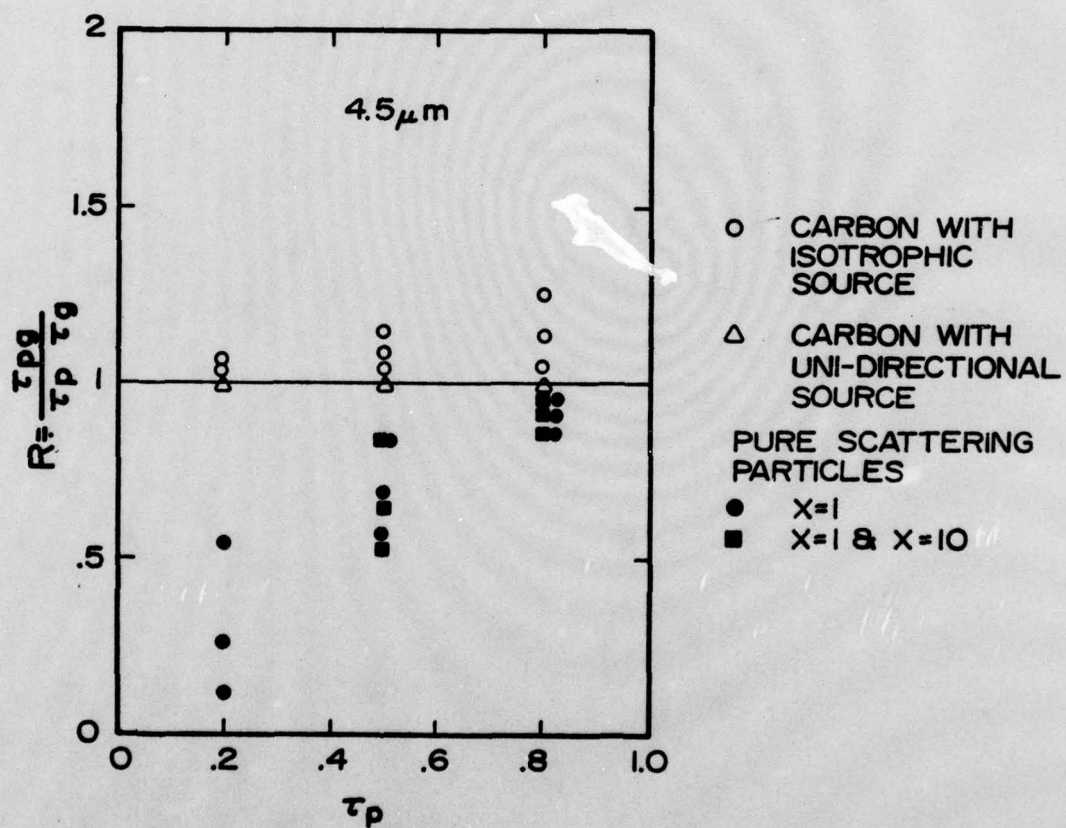


Fig. 6. Synergistic ratio for pure scattering particles and N_2O mixture and carbon- N_2O mixture.

carbon particles of sizes $x = .1, 1, \text{ and } 10$ in N_2O to determine possible synergistic effects due to scattering. The synergistic ratio, defined earlier, for some of these calculations are plotted in Figure 6, and show that the carbon scattering does not increase the net radiation loss by the N_2O gas. The absorption within the carbon particle is too great. This absorption is illustrated in Figure 7 where transmission versus mass density for three different particles sizes is plotted. Remember this represents transmission through a one-kilometer slab having the uniform mass density indicated. It is most interesting to see that $x = 1$ is a preferred particle size. This is due to the fact that the scattering coefficient attains a maximum value near $x = 1$.

The effectiveness of carbon particles in infrared obscuration is indicated in Figure 8. IR transmission at $4.5\mu\text{m}$ through both carbon and N_2O is plotted versus weight. It is easily seen that much less carbon is required for a given transmission value even though the particles are much bigger than molecules.

III. EXPERIMENTAL EFFORT

A. Experimental Procedure

The apparatus used for these measurements was identical to that used in the previous work [Harris et al., 1975] on gaseous absorbers, with one exception: the gas absorption cell was replaced by a scattering/absorbing chamber. This chamber was a small plexiglass cube (2" inside dimension) fitted with sapphire windows on two opposing faces. A small electric motor was mounted on the outside of the top face. The motor shaft extended downward through the box and drove a multi-bladed fan fitted to the end of the motor shaft. Additionally, a magnetic stirring bar was placed on the floor of the chamber and driven by a magnetic stirring motor from the bottom. The combination of fan and stirring bar provided a reliable means of maintaining reasonably uniform particle suspensions within the chamber. Neither the fan nor stirring bar interfered with the direct optical line of sight through

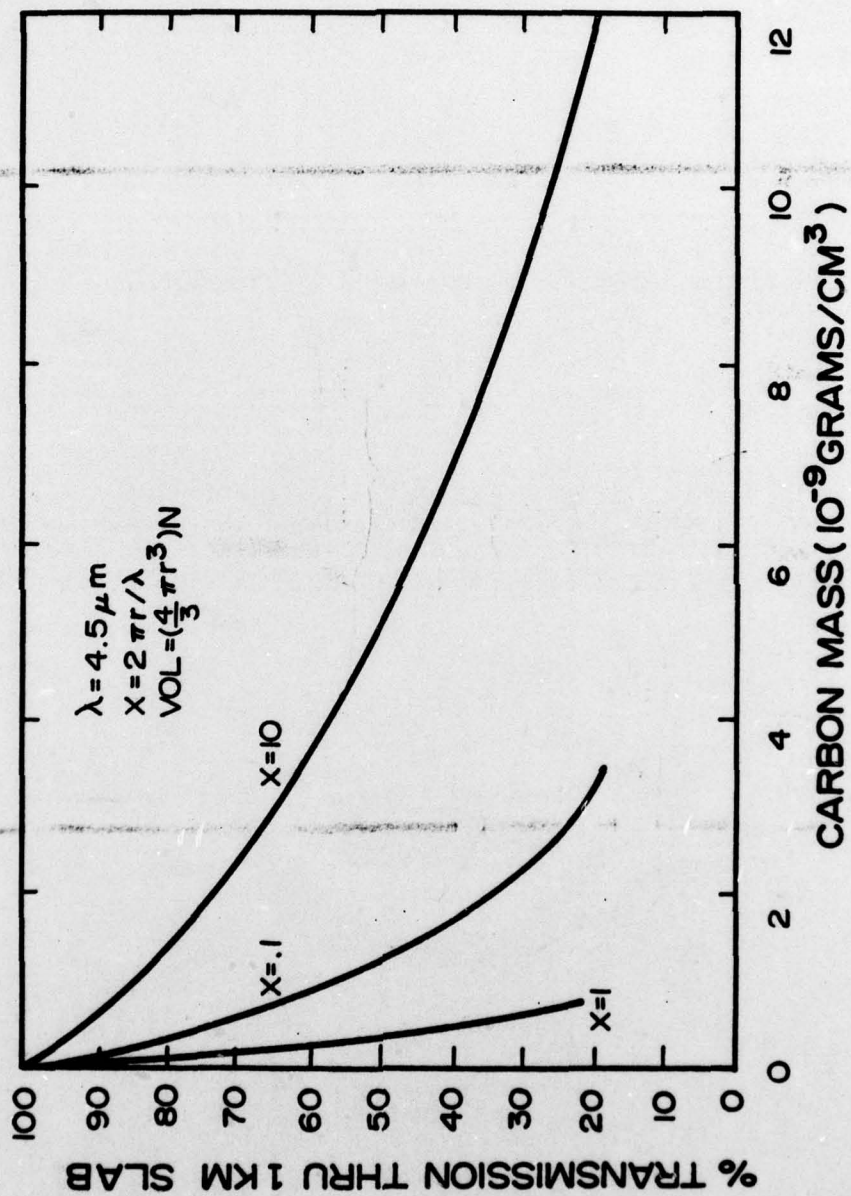


Fig. 7. Transmission through 1 km slab of carbon particles.

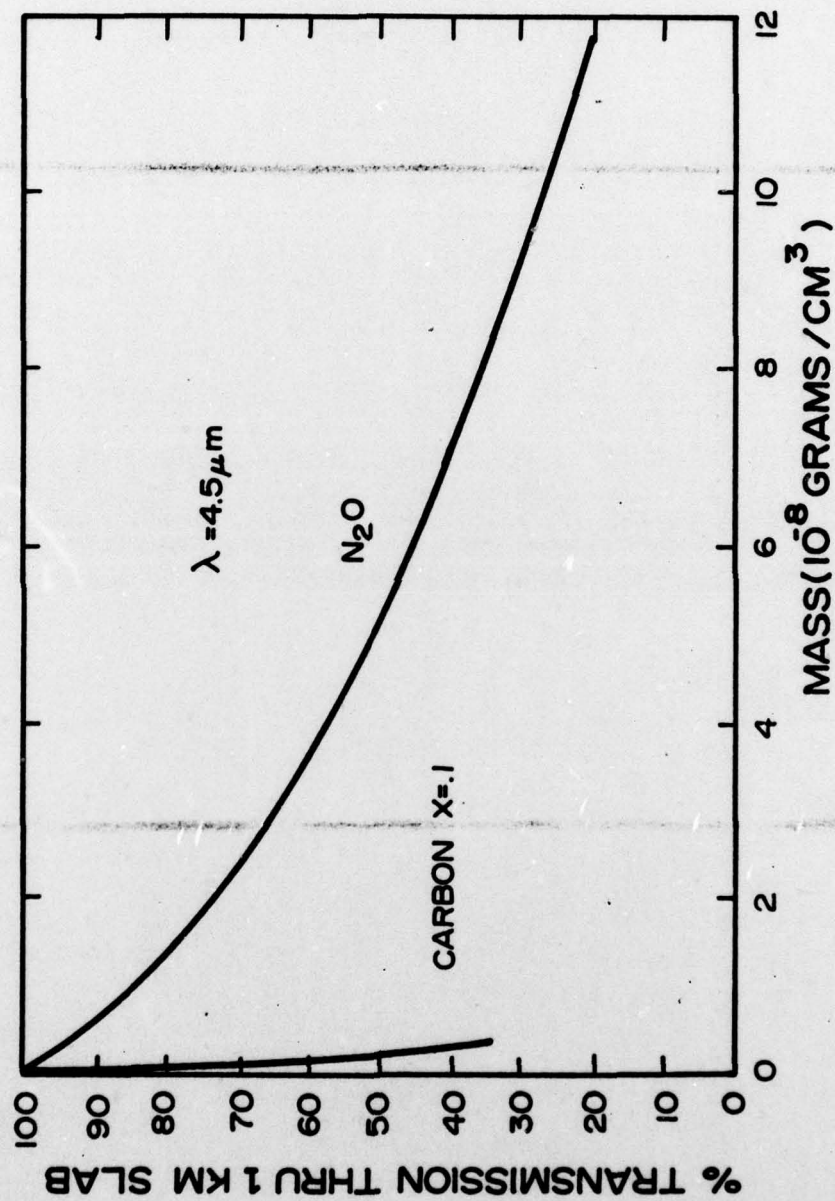


Fig. 8. Comparison of carbon and N_2O transmissions versus weight of absorber.

the chamber. Early attempts to suspend the particles with an ultrasonic particle disrupter unit did not meet with success. The worst defect of this method was the generation of standing wave patterns in the chamber with the result of highly non-uniform particle distributions. In one columnar chamber design, for example, the particles noticeably collected at the wave nodes.) No quantitative measure of particle number density was made. This parameter is eliminated in the method of analysis used (described later) and is not required. Crude estimates of maximum density obtainable in the chamber were made by noting visually the largest amount of material that could be maintained off the floor of the chamber. This maximum was approximately 0.001 g/cm^3 . Two copper tubes through the top of the chamber were used to flush in N_2O and N_2 gases. The radiation source, chopper, atmospheric simulation, monochrometer, detector and display apparatus were the same as used in the previous work, [Harris et al., 1975].

Particles used in the measurements included carbon in the size category 0.1 to $0.66 \text{ }\mu\text{m}$ diameter ($0.32 \text{ }\mu\text{m}$ average, $x = .22$ at $4.5 \mu\text{m}$) and 3 to $8 \text{ }\mu\text{m}$ diameter ($6 \text{ }\mu\text{m}$ average), and $2 \text{ }\mu\text{m}$ diameter TiO_2 .

Data were taken for three conditions in the scattering chamber:

- 1) chamber empty (flushed with N_2)
- 2) N_2O alone
- 3) particles in N_2O .

Typical spectral results in the $4.6 \text{ }\mu\text{m}$ region are shown in Figures 9 and 10. The data were analyzed on a whole-band basis by measuring areas under the various curves. Measurements for conditions 1 and 2 provide the transmission data for N_2O alone. Measurements for conditions 2 and 3 provide, simultaneously, the transmission data for scatterers alone and scatterers and absorption gas in combination. This was accomplished by determining the transmissions separately in the $4.2 \text{ }\mu\text{m}$ spike and the 4.3 to $4.7 \text{ }\mu\text{m}$ wing. Since there is no absorption due to N_2O in the $4.2 \text{ }\mu\text{m}$ region, measurements on this spike provide a measure of attenuation due to scatterers alone. This measure of particle attenuation is

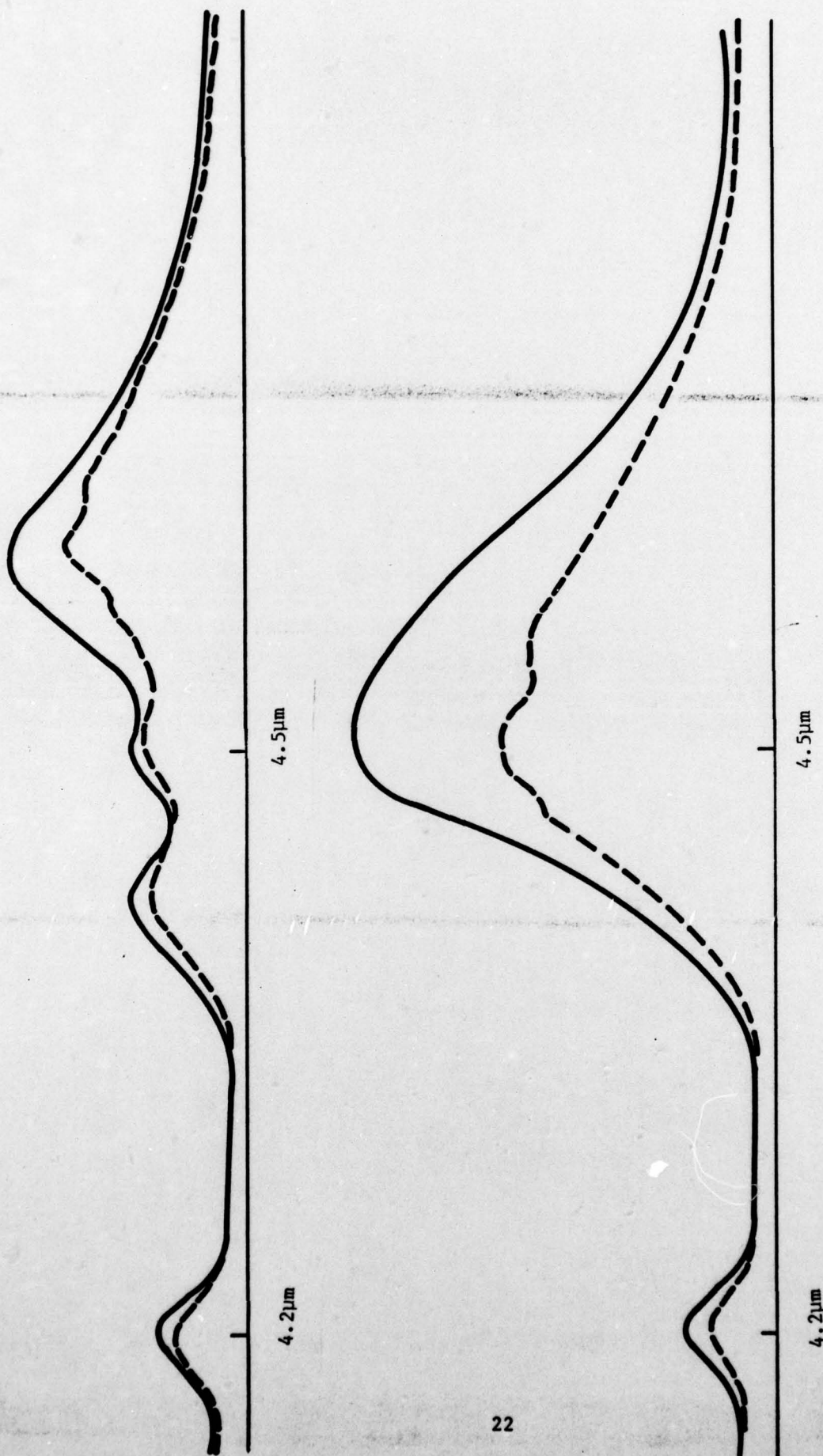


Fig. 9. Upper spectrum, solid curve, is 4.1 to 4.8 micron region of flame as seen through the CO_2 atmospheric path simulator (sea level, 1200ft.) with 20 torr partial pressure of N_2O in scattering cell. Dashed curve is for N_2O plus suspended carbon. Lower spectrum is for same region and same path length simulation with nitrogen in scattering cell (solid curve) and nitrogen plus suspended carbon (dashed curve).

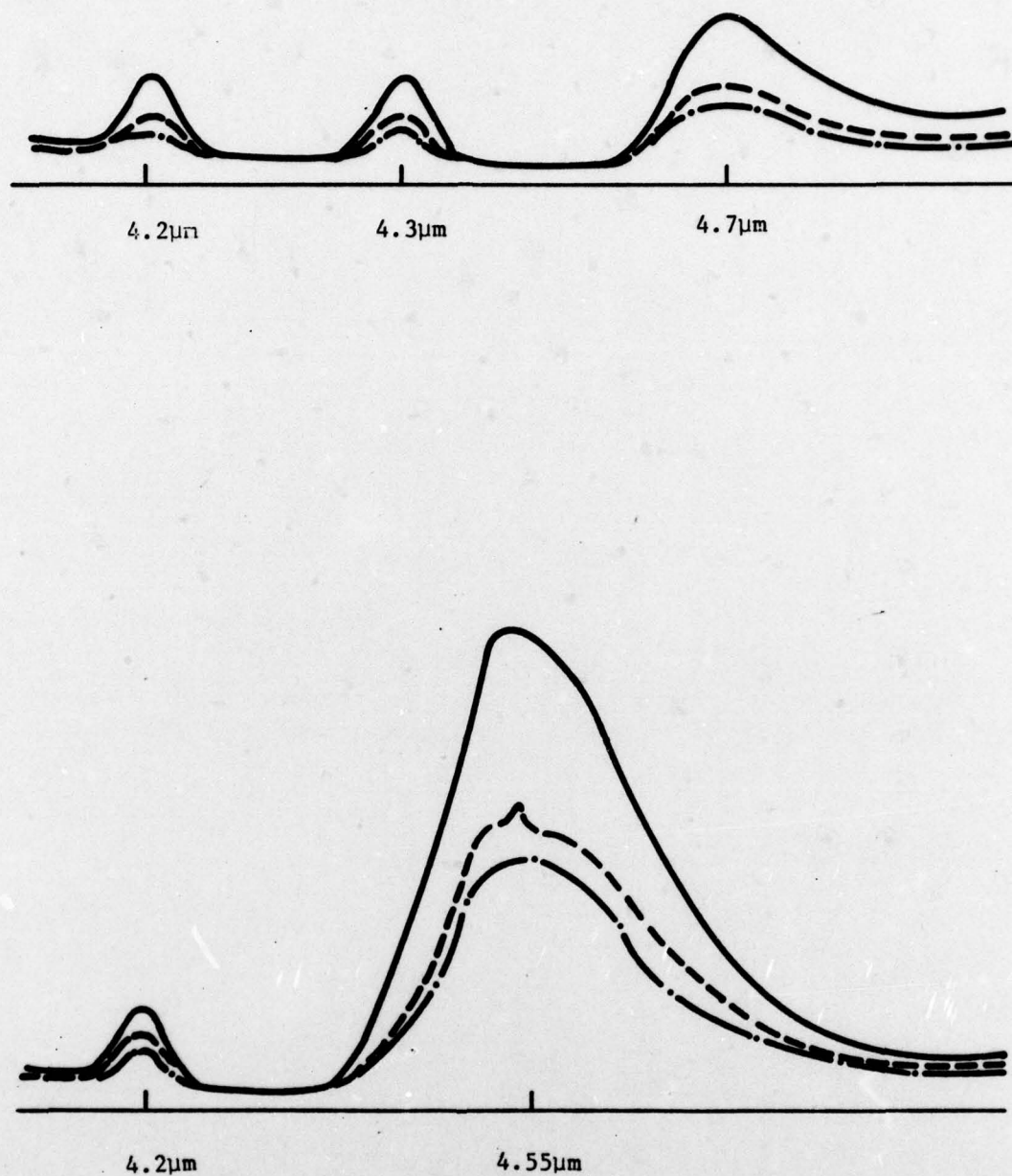


Fig. 10. Upper spectrum, solid curve, is 4.1 to 4.8 micron region of flame as seen through CO₂ atmospheric path simulator (sea level, 1200ft.) with 600 torr partial pressure of N₂O in scattering cell. Dashed curves are for two different concentrations of carbon in the N₂O mixture. Lower spectrum is for the same region and same path length simulation with nitrogen in scattering cell (solid curve) and nitrogen plus two different concentrations of suspended carbon (dashed curves).

assumed to prevail throughout the entire band spectral region. (Preliminary measurements of particle attenuation had been made by suspending the particles in N_2 . It was discovered, however, that for fixed stirrer power levels, that N_2 and N_2O would not suspend the same amount of material.) Measurements on the 4.3 to 4.7 μm wing provide the measure of attenuation due to particles and N_2O in combination.

Let τ_g be the measured transmission of the N_2O alone (mean value over whole band), τ_p be the measured transmission due to particles alone (mean value in 4.2 μm spike), and τ_{pg} be the measured transmission due to particles and N_2O in combination (mean value in 4.3 to 4.7 μm wing).

3. Experimental Results

Results for the synergism ratio R are presented in Figures 11 and 12 for the 0.3 μm carbon sample and the 2 μm TiO_2 sample, respectively. The plotting abscissa for these figures is the particle-alone transmittance τ_p . To within the experimental uncertainty, the ratio R is unity for all optical depths. The scatter of the data is quite large and could conceivably hide a synergism of less than $R = 0.9$ for carbon (none for TiO_2). However, this amount of synergism would not be significant in the overall plume obscuration scheme.

Data obtained in the 2.9 μm region and data for other particle size groups were too scattered and incomplete for presentation. Given the negative result of Figures 11 and 12, it was felt that no purpose would be served by spending time on improving that data.

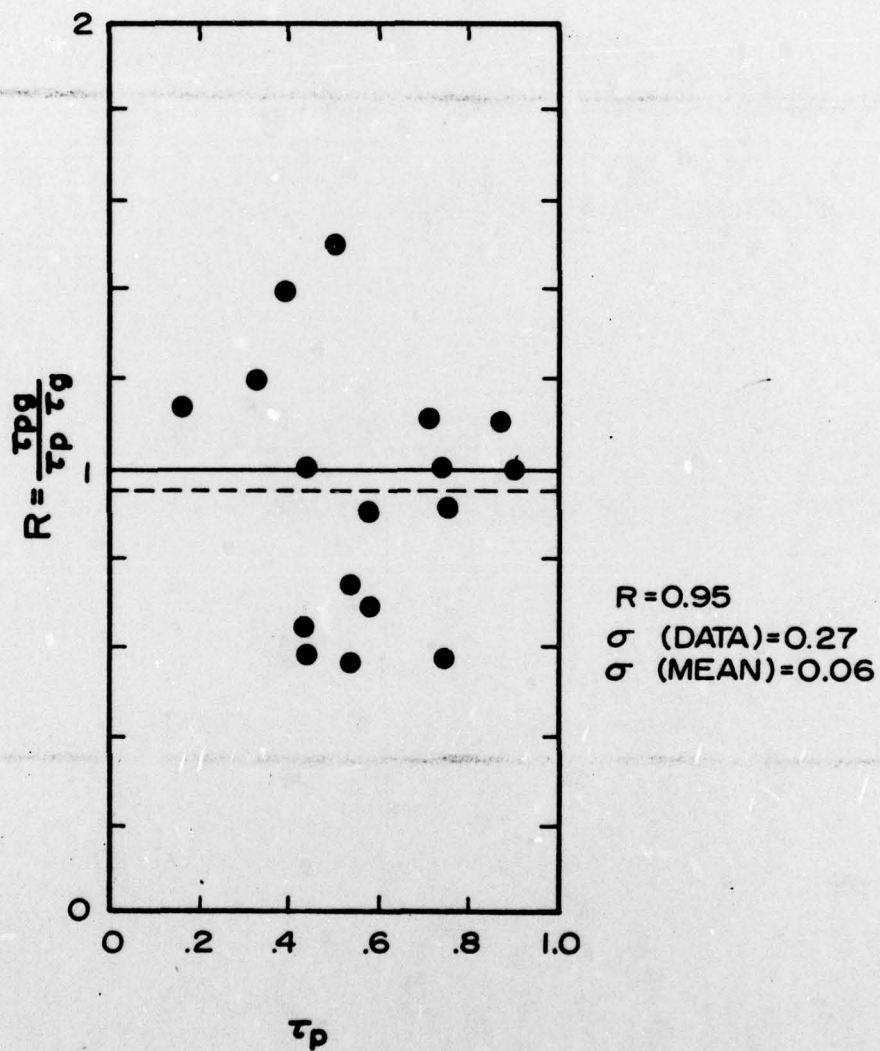


Fig. 11. Synergism ratio for $0.3\mu\text{m}$ carbon sample in the $4.3\mu\text{m}$ spectral region.

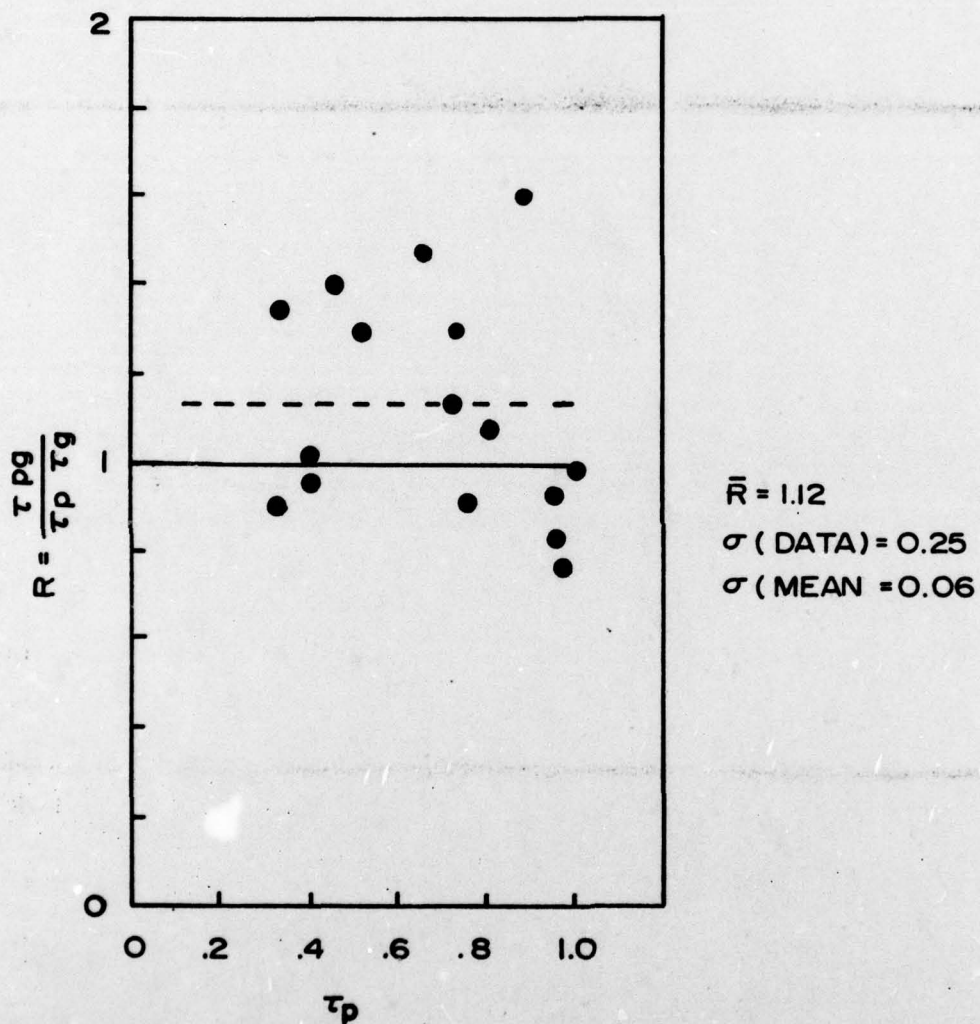


Fig. 12. Synergism ratio for 2.0 μm TiO_2 sample in the 4.3 μm spectral region.

IV. CONCLUSIONS

A study was conducted to evaluate the role of scattering particles in the absorption of infrared radiation through an aerosol-absorbing gas mixture. The study incorporated both theoretical and experimental methods. Theoretical calculations of IR radiation transport through scattering/absorbing mediums were made with a computer code obtained from Lawrence Radiation Laboratories and modified by us. Experimental measurements were made of IR flame spectra transmitted through cells filled with scattering particles and/or absorbing gases. The results of these two efforts are consistent and may be summarized as follows:

- 1). Both theoretical and experimental results show that synergistic effects in media containing pure scatterers and absorbing gas is small, not greater than about 10%. Titanium dioxide was used for the scattering medium and N_2O the absorbing gas because of its absorption effectiveness in the red wings of the 2.7 and 4.3 μm bands.
- 2). Theoretical and experimental results also showed that synergistic effects in a medium containing carbon and N_2O was again small, less than 10%. Carbon particles both scatter and absorb internally infrared radiation.
- 3). In the light of conclusions 1 and 2, we regretfully conclude that augmented absorption produced by scattering particles in an absorbing medium is not a viable technique for infrared observation in exhaust plumes.
- 4). Carbon particles produce strong infrared absorption. The internal absorption coefficient is about 10^3 higher than the scattering coefficient. Because the absorption is particle-like, there is less structure in the absorption-versus-frequency response than in a gaseous absorber like N_2O . Carbon absorption at 2.7 μm is only a factor of 2 less than that at 4.3 μm . Furthermore, it was shown at 4.5 μm that a greater weight of N_2O was required to achieve a given IR absorption than with carbon. Except for the black color in the visible, black carbon is an attractive substance for hot plume obscuration.

V. REFERENCES

1. Birstein, S.J., "The Successful Testing of an Operationally Feasible System for Infrared Suppression - Pave Shield Final Report (U)," AFCRL Report TR-76-0007, January 1976 (Secret).
2. Blozy, J.T., "Calculations and Analysis of Infrared Suppression Capabilities of an Off-On System (U)," Paper presented at the 12th IRIS Symposium on Infrared Countermeasures, Ft. Monmouth, N.J., 3-4 April 1974.
3. Born, M. and E. Wolf, "Principal of Optics" fourth edition, Pergamon Press, 1970.
4. Braslau, N. and J.V. Dave, "Effect of Aerosols on the Transfer of Solar Energy Through Realistic Model Atmospheres. Part I: Non Absorbing Aerosols", J. Appl. Meteorology, 12, pp. 601-614, June, 1973.
5. Caldwell, D. private communication, 1975.
6. Chandrasekka, S., "Radiative Transfer", Rover Publications Inc., 1960.
7. Chu, C.M. and S.W. Churchill, "Presentation of the Angular Distribution of Radiation Scattered by a Spherical Particle", J. Opt. Soc. Amer., 45, pp 958-962, Nov, 1955.
8. Dave, J.V., "Coefficients of the Legendre and Laurier Series for the Scattering Functions of Spherical Particles", Appl. Optics, 9, pp 1888-1896, Aug., 1970.
9. Dave, J.V., "Development of Programs for Computing Characteristics of Ultraviolet Radiation. Technical Report-Scalar Case", IBM report for NASA, Contract No. NAS5-21680, May, 1972.
10. Dave, J.V. and J. Gazdaz, "A modified Lourier Transform Method for Multiple Scattering Calculations in a Plane Parallel Mie Atmosphere", Appl. Optics, 9, pp 1457-1466, June, 1970.
11. Deirmendjian, D., "Electromagnetic Scattering on Spherical Polydispersions", American Elsevier Publishing Co., 1969.
12. Harris, R.D., W.R. Pendleton, S.J. Young and L.R. Martin, "Evaluation of the Absorbing Shroud Concept of the Aircraft Plume Radiation Obscuration in the Infrared", Utah State University Final Report for Department of Navy, Naval Air Systems Command, Contract No. N00019-73-C-0384, June, 1975.

13. Luther, F.M., "Solar Radiation Model RADI", Lawrence Livermore Laboratory Report No. UCID-16572, August, 1974.
14. Mie, G., Am. Phys., 25, pp 377, 1908
15. Sekera Z., "Legendre Series of the Scattering Functions for Spherical Particles", Rep. No. 5, Contract No. AF199(122)-239, Department of Meteorology, Univ. of Calif., Los Angeles, Calif. ASTIA No. AD-3870, 1952.
16. Van De Hulst, H.C., "Light Scattering by Small Particles", John Wiley and Sons, Inc, 1957.
17. Varney, G.E., "Suppression Concepts Study (U), "General Electric Report 72AEG72, December 1972 (Secret).
18. Whitson, M.E. Jr., "Handbook of the Infrared Optical Properties of Al_2O_3 , Carbon, MgO , and ZrO_2 , Aerospace Corp. Technical Report TR-0075 (5548)-2⁸, Vol. I, Los Angeles, Calif., 4 June, 1975.